

## Coupling of two-quasiparticle and collective excitations in Ge and Zn isotopes

M. Didong, H. Mütter, K. Goeke, and Amand Faessler\*

*Institut für Kernphysik der Kernforschungsanlage Jülich, D-5170 Jülich, West Germany*

(Received 5 April 1976)

Excitation energies and  $B(E2)$  values of  $^{72}\text{Ge}$ ,  $^{70}\text{Zn}$ , and  $^{74}\text{Ge}$  are investigated by means of an extended generator coordinate method which allows in a microscopic way a simultaneous coupling of single particle and collective degrees of freedom. For the generating wave functions angular momentum and particle number projected Hartree-Fock-Bogoliubov solutions have been used. The low lying states of even parity and angular momentum are dominated by a coupling of shape vibrations and  $K = 0$  two-quasiparticle excitations. In contrast to the yrast states especially the anomalously low lying first excited  $0^+$  state in  $^{72}\text{Ge}$  could only be explained by a strong coupling of both degrees of freedom. For  $^{72}\text{Ge}$  and  $^{74}\text{Ge}$ , the most important contributions are due to the proton excitations, whereas in  $^{70}\text{Zn}$ , the neutron excitations play the dominant role.

NUCLEAR STRUCTURE Calculations in Ge and Zn; generator coordinate method; Hartree-Fock-Bogoliubov approach; angular momentum projection; two-quasiparticle states.

### I. INTRODUCTION

With the introduction of the generator coordinate method (GCM) by Griffin, Hill, and Wheeler,<sup>1</sup> physicists had a very flexible tool to describe in a microscopic way the nuclear collective motion, as for instance quadrupole vibrations, pairing vibrations, and rotational-like excitations.<sup>2-4</sup> Now, the GCM theory can be generalized to consider, apart from collective degrees of freedom, also single particle degrees of freedom. A coupling of both can be achieved by a supplementary term to the general GCM ansatz of the nuclear wave function, containing states which are either particle-hole or two-quasiparticle excited configurations<sup>5</sup> (GCM+QP).

Nuclei which are especially adopted for a GCM treatment are, for instance, those far away from closed shells such that shell model techniques are no longer applicable without too severe truncations of the configuration space. A particular interest for the use of GCM+QP may be attributed to those nuclei which exhibit excitation spectra showing collective as well as noncollective effects. Suitable examples for medium heavy nuclei exist in the mass region  $A \approx 70$ , where one of the most promising candidates is the  $^{72}\text{Ge}$  isotope, which shows in addition to other anomalies a deep lying first excited  $0^+$  state at about 0.7 MeV. Other nonmagic nuclei with this feature are  $^{90}\text{Zr}$  and  $^{98}\text{Mo}$ . These first excited states are in complete conflict with any vibrational picture, although the ratio  $E(4^+)/E(2^+)$  indicates a tendency for the validity of the vibrational model in these nuclei.

First attempts to understand those nuclei were done by Kregar and Mihailovic<sup>6</sup> who used the Davydov nonadiabatic model, assuming that the first excited  $0^+$  states in the region of Ge and Se isotopes correspond to the oblate "ground state." The real ground state itself should belong to the prolate shape of small axially symmetric deformation. In the special case of  $^{72}\text{Ge}$ , this model could not explain the puzzling  $0^+$  state which came out too high in energy.

In recent time the low lying spectrum of  $^{72}\text{Ge}$  has been investigated by Castel, Micklinghoff, and Johnstone.<sup>7</sup> In analogy to the work of Bayman *et al.*,<sup>8</sup> who studied  $^{90}\text{Zr}$  in terms of a pair configuration for the two valence protons occupying the  $p_{1/2}$  and  $g_{9/2}$  orbitals, they performed a shell model calculation for the two valence neutrons and considered in addition the coupling of these neutrons to the observed collective excitations of the  $^{70}\text{Ge}$  core. Furthermore, they included also excitations from the  $p_{1/2}$  and  $f_{5/2}$  subshells by introducing second order perturbation diagrams. With a two parameter fit, they got a good agreement with experiment.

The success of this semimicroscopic model<sup>7</sup> and especially the importance of single particle degrees of freedom suggested that it should be possible to describe  $^{72}\text{Ge}$  in a fully microscopic way, where the collective and single particle degrees of freedom are taken into consideration by the use of microscopic wave functions, which are superimposed to give rise to the GCM+QP ansatz, discussed in more detail in the next section.

The formalism of GCM+QP is also applied to  $^{74}\text{Ge}$  and  $^{70}\text{Zn}$  to see how important single particle

degrees of freedom are in the vicinity of  $^{72}\text{Ge}$ . In the case of  $^{70}\text{Zn}$ , we meet again a relatively low lying first excited  $0^+$  which is situated slightly above the first excited  $2^+$  but still not high enough to be explained by the vibrational model.

Section II reviews the GCM+QP theory leading to the solution of a coupled set of integral equations. Because of the strong pairing correlations of the considered nuclei we used HFB states with a given deformation as generating wave functions. Before entering the integral equations mentioned above, these wave functions are to be projected on good angular momentum and particle number in order to restore symmetries and remove spurious components which are known to effect noticeably the excitation energies.<sup>9</sup> The section is closed by some numerical details and is followed by the discussion of the most important results in Sec. III. The last section finally contains a short summary and some conclusions.

## II. THEORY AND NUMERICAL DETAILS

Starting from a many body Hamiltonian the generator coordinate method (GCM) describes the collective degrees of freedom of nuclear motion on a purely microscopic level. In order to go beyond the description of just the collective motion by including also single particle degrees of freedom, one has to extend the general GCM ansatz of the nuclear wave function by one or few particle excited configurations.

In principle the GCM and GCM+QP procedures consist of choosing suitable basis vectors with different physical properties, appropriate to the problem in study, and selecting in this way out of the Hilbert space a subspace, where a total nuclear wave function is spanned by superposition of the chosen basic states which are not necessarily orthonormal. The generator coordinates are, for instance, the quadrupole moment  $Q$ , a variation of which gives rise to shape vibrations, or the orientation  $\Omega$  of the deformed nucleus, responsible for the rotational degrees of freedom. In GCM+QP there are taken into account, in addition to GCM, also quasiparticle excitations on the generating wave functions which allow one to take care of specific single particle excitations.

Because the nuclei in the mass region  $A \approx 70$  show somehow vibrational features, the ansatz for the total GCM+QP wave function for the nuclei to be considered has the form

$$|\psi_J\rangle = \int d\beta f(\beta) \hat{P}_J \hat{Q}_N |\phi(\beta)\rangle + \sum_i \int d\beta f^i(\beta) \hat{P}_J \hat{Q}_N |\phi^i(\beta)\rangle. \quad (1)$$

In this ansatz  $|\phi(\beta)\rangle$  are self-consistent Hartree-Fock-Bogoliubov (HFB) functions depending on the deformation  $\beta$ . These wave functions are obtained by solving the constrained HFB equations, where the Hamiltonian is written as  $\hat{H} = \hat{H} - \lambda \hat{N} - \mu \hat{Q}$ . The  $\hat{N}$  and  $\hat{Q}$  are the particle number and the quadrupole operators, respectively. The second term in (1) contains two-quasiparticle excited HFB states, depending on the deformation  $\beta$ . The index  $i$  denotes the two-quasiparticle excitations

$$|\phi^i(\beta)\rangle = a_i^\dagger a_i^\dagger |\phi(\beta)\rangle, \quad (2)$$

where  $a_i^\dagger$  and  $a_i^\dagger$  are the quasiparticle creation operators defining the HFB states  $|\phi(\beta)\rangle = \prod_i a_i |0\rangle$ .

The HFB states  $|\phi(\beta)\rangle$  and the two-quasiparticle states  $|\phi^i(\beta)\rangle$  are projected onto good angular momentum  $J$  and particle number  $N$  by means of the projection operators  $\hat{P}_J$  and  $\hat{Q}_N$ ,

$$\hat{P}_{JM} = \frac{2J+1}{8\pi^2} \sum_K \int d\Omega D_{MK}^{J*}(\Omega) \hat{R}(\Omega), \quad (3)$$

$$\hat{Q}_N = \frac{1}{2\pi} \int_0^{2\pi} d\vartheta \exp[i(N-N)\frac{1}{2}\vartheta]. \quad (4)$$

The variational principle  $\delta \langle \psi_J | \hat{H} - E | \psi_J \rangle = 0$  determines the unknown expansion coefficients  $f(\beta)$  and  $f^i(\beta)$  in (1). This leads to a set of coupled integral equations:

$$\int d\beta_1 f(\beta_1) \langle \phi_J(\beta_2) | \hat{H} - E | \phi_J(\beta_1) \rangle + \sum_j \int d\beta_1 f^j(\beta_1) \langle \phi_J(\beta_2) | \hat{H} - E | \phi_J^j(\beta_1) \rangle = 0, \quad (5)$$

$$\int d\beta_1 f(\beta_1) \langle \phi_J^i(\beta_2) | \hat{H} - E | \phi_J(\beta_1) \rangle + \sum_j \int d\beta_1 f^j(\beta_1) \langle \phi_J^i(\beta_2) | \hat{H} - E | \phi_J^j(\beta_1) \rangle = 0.$$

The usual Hill-Wheeler equation appears as an approximation of these equations if one omits the terms corresponding to the single particle degrees of freedom. In practical calculations the integrals in (1) and (5) must be made discrete so that a finite number of generating wave functions  $|\phi(\beta)\rangle$  and  $|\phi^i(\beta)\rangle$  are used. The solution of system (5) then consists of a diagonalization of the Hamiltonian in the nonorthogonal basis. The non-orthogonality of the overlap matrix elements takes care of the linear dependence of the basis states.

In the present calculations we restricted ourselves to axial symmetric HFB states with  $K=0$ . This has the advantage that the angular momentum projection operator  $\hat{P}_{JM}$  can be simplified to

$$\hat{P}_J = \frac{2J+1}{2} \int_0^\pi d\alpha \sin\alpha d_{00}^J(\alpha) \hat{R}(\alpha). \quad (6)$$

Furthermore, we select pairs of time conjugated quasiparticle excitation operators  $a_i^\dagger a_i^\dagger$  in Eq. (2). The use of those  $K=0$  quasiparticle excitations has the advantage that the two-quasiparticle states can be written as a product of quasiparticle annihilation operators acting on the vacuum so that the numerical methods of the evaluation of the norm and energy overlap matrix elements can be applied just as for the normal HFB states. The restriction to  $K=0$  quasiparticle states only may be justified because the lowest two-quasiparticle state is of this form. In addition the low lying excitation spectrum should be dominated by  $K=0$  configurations.

With all these simplifications which reduce to a great amount the numerical effort, an energy overlap matrix element can be written:

$$\begin{aligned} & \langle \phi_J(\beta_2) | \hat{H} | \phi_J(\beta_1) \rangle \\ &= \int d\beta d\vartheta d_{00}^{J*}(\beta) \sin\beta \int d\vartheta \exp(-i\frac{1}{2}N\vartheta) h_{12}(\beta, \vartheta) \end{aligned} \quad (7)$$

with

$$h_{12}(\beta, \vartheta) = \langle \phi(\beta_2) | \hat{H} \hat{R}(\beta) \hat{S}(\vartheta) | \phi(\beta_1) \rangle. \quad (8)$$

The detailed formulas for this overlap and the norm overlap can be found in Ref. 10.

The model space for the HFB functions is spanned by eigenfunctions of the three-dimensional harmonic oscillator. Our basis includes the  $1p_{3/2}$ ,  $0f_{5/2}$ ,  $1p_{1/2}$ , and  $0g_{9/2}$  shells, assuming  $^{56}\text{Ni}$  as an inert core. Furthermore, we allow only  $T=1$  pairing for protons and neutrons, respectively, an assumption which is known to be valid for  $N>Z$  nuclei. Coulomb, center-of-mass, and isospin corrections are not taken into account.

As a nucleon-nucleon force we used the "modified surface  $\delta$  interaction" (MSDI)

$$V_{ij} = 4\pi A_T \delta(\Omega_{ij}) \delta(\Omega_i - R) \delta(\Omega_j - R) + B(\tau_i \cdot \tau_j) \quad (9)$$

depending on the isospin  $T$ .

The parameters  $A_T$  and  $B$  as well as the single particle energies  $\epsilon$  have been given by Glaudemans *et al.*<sup>11</sup> The values for these parameters are  $A_1=0.35$ ,  $A_0=0.43$ ,  $B=0.33$ , and the single particle energies are

$$\begin{aligned} \epsilon(1p_{3/2}) &= 0.0 \text{ MeV}, & \epsilon(0f_{5/2}) &= 1.75 \text{ MeV}, \\ \epsilon(1p_{1/2}) &= 2.20 \text{ MeV}, & \epsilon(0g_{9/2}) &= 3.39 \text{ MeV}. \end{aligned}$$

### III. RESULTS AND DISCUSSION

In order to get a first idea about the vibrational degrees of freedom in  $^{72}\text{Ge}$ , the intrinsic defor-

mation energy surface has been calculated. The total binding energy surface  $\langle \phi(\beta) | \hat{H} | \phi(\beta) \rangle$  for the nonprojected HFB states is displayed in Fig. 1 (dashed line). The curve shows a very flat valley around the spherical minimum so that it is not possible to attribute a certain deformation to the nucleus. Nonetheless, one can conclude that  $^{72}\text{Ge}$  is a rather soft and weakly deformed nucleus.

An analogous independence of energy on small deformations is shown in Fig. 2, where the pairing energies for neutrons, the one for protons and the total pairing energies

$$\Delta = \frac{1}{2} \sum_{i k m n} V_{i k m n} \langle c_i^\dagger c_k^\dagger \rangle \langle c_n c_m \rangle \quad (10)$$

are given. The order of magnitude of the total pairing energy ( $\approx -7$  MeV) makes the use of HFB states rather than HF states indispensable. This has been verified by using also HF states where the total intrinsic energies are about 1 to 3 MeV smaller. Even by a superposition of a few Slater determinants we could not account of all the cor-

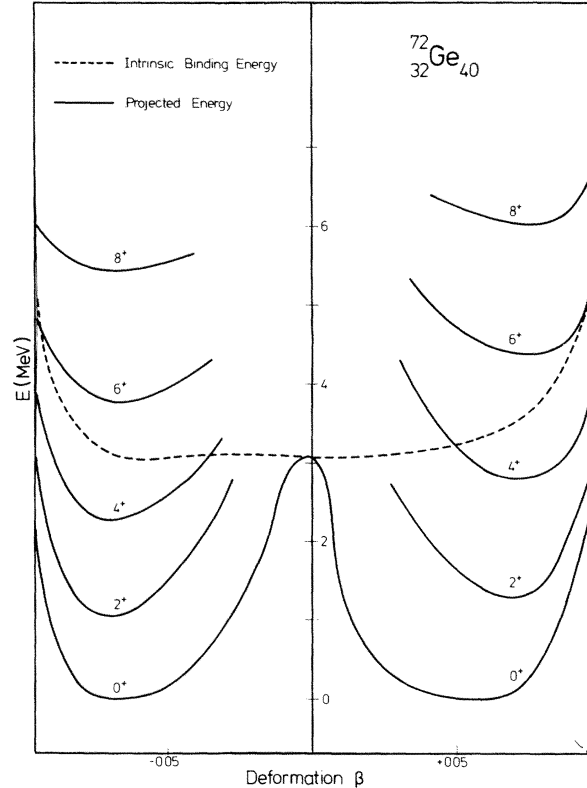


FIG. 1. Intrinsic binding energies  $\langle \phi(\beta) | \hat{H} | \phi(\beta) \rangle$  (dotted line) and the binding energies of angular momentum and particle number projected wave functions  $\langle \phi_J^N(\beta) | \hat{H} | \phi_J^N(\beta) \rangle$  are plotted as a function of the deformation  $\beta$ .  $|\phi(\beta)\rangle$  are axial symmetric HFB states constraint on a given deformation  $\beta$ .

relations of the HFB functions.

The different energy surfaces discussed so far allow a very rough estimate of the connection between energies and deformations. But they are no longer suitable for a detailed treatment since the intrinsic HFB wave functions violate angular momentum and particle number conservation. Therefore we consider now the binding energies given by angular momentum and particle number projected HFB states. The corresponding surfaces are visualized by the full lines in Fig. 1. In contrast to the flat intrinsic binding energy surface, they have distinct minima for roughly all spins at deformations  $\beta \approx \pm 0.07$ . This behavior may slightly be changed when another effective Hamiltonian is used, but one can learn that a careful study of the projected energy surface is important rather than to look to the intrinsic properties only.<sup>12</sup> The minima of the angular momentum projected energy surfaces shown in Fig. 1 yield the first spectrum of Fig. 3. One sees immediately that the spectrum projected before  $\beta$  variation (PHFB) does not follow the  $J(J+1)$  law of the pure rotator model because of the small deformation.

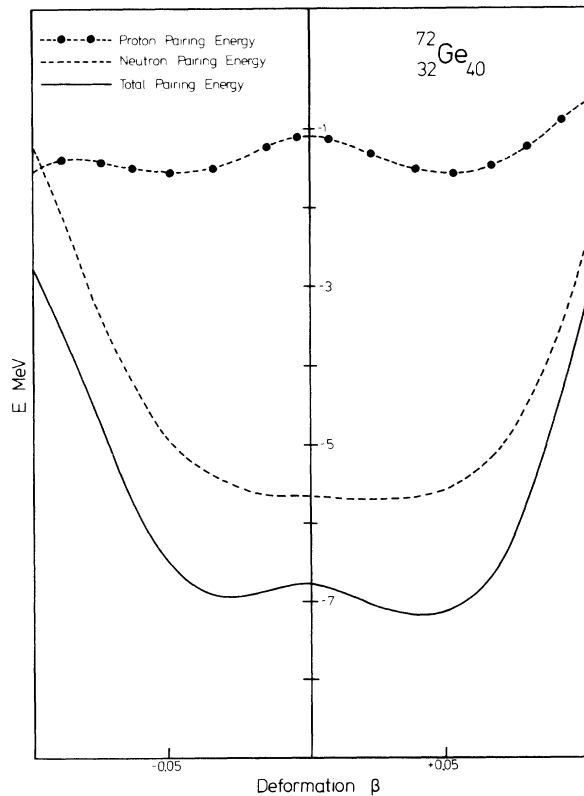


FIG. 2. Proton pairing energies (upper curve), neutron pairing energies (middle curve), and the total pairing energies of HFB wave functions are plotted against the deformation  $\beta$ .

For the following application of GCM, it is reasonable and consistent with the minimization principle to rely upon those HFB states whose projected spectra exhibit already energetic minima on either side (Fig. 1). It has been shown that in many cases the vibrational degrees of freedom are sufficiently well described by a superposition of projected wave functions corresponding to those prolate and oblate minima only.<sup>4</sup> The results of such a prolate/oblate mixing can be found in the second column of Fig. 3 ( $\beta$ -GCM). Compared with the first spectrum (Fig. 3, PHFB) the first  $0^+$  and  $2^+$  states are lowered by 0.15 to 0.25 MeV, whereas the  $4^+$  and  $6^+$  are nearly not affected. But the first excited  $0^+$  still lies too high in energy. This may be explained by the fact that the two prolate-oblate states projected on  $J=0^+$  have an overlap of 45% only. Therefore the energy difference between the two  $2^+$  states is smaller than for the  $0^+$  states. Additional generator functions with different deformations did not change very much the given spectrum ( $\beta$ -GCM) which means that one can assume to have taken into account the most important vibrational degrees of freedom by mixing only prolate and oblate deformed HFB states.

In order to increase the model space we include also quasiparticle degrees of freedom by using the two-quasiparticle excited HFB states [Eq. (2)]. The states  $i$  defined in the excitation operator  $a_i^\dagger a_i^\dagger$  are those lying in the neighborhood of the Fermi surface  $E_F$ . The HFB functions on which the creation operators act are the prolate and oblate states described above. The quasiparticle energy levels for those two functions are given in Fig. 4. The important quasiparticle levels are for the protons in the prolate case the  $p_{3/2, \Omega=3/2}$  and  $f_{5/2, 1/2}$ , in the oblate case the  $p_{3/2, 1/2}$  and  $f_{5/2, 5/2}$ . For neutrons, the only important level was the prolate  $p_{1/2, \Omega=1/2}$ . Other excited HFB states have been tested, but their contribution to the final spectrum turned out to be negligible.

Now GCM+QP calculations are performed using different sets of generating wave functions. The results are given in Fig. 3. In the third column [2qp (oblate)] only oblate states are taken into account. Compared with the previous one ( $\beta$ -GCM) all levels are higher in energy. Therefore, we couple now all available proton quasiparticle excited states to the simple prolate and oblate deformed states. The resulting GCM+QP function produces the spectrum in the fourth column of Fig. 3 [ $\beta$ -GCM+2qp (proton)]. Here, all energy levels are lowered, compared with the previous spectra. Especially the second  $0^+$  has come down by more than 1 MeV and is lying now below the first  $2^+$  state, in agreement with the experimental sequence. In the next to last spectrum ( $\beta$ -GCM

+2qp) the remaining neutron component has been added, but it does not affect noticeably the low lying spectrum. This spectrum is represented by the total nuclear wave function which will be analyzed in more detail in Table I, where the overlaps  $|\langle \psi | \phi(\beta) \rangle|^2$  and  $|\langle \psi | \phi^i(\beta) \rangle|^2$  for  $J=0_1^+$  and  $0_2^+$  are listed. One sees that for the ground state, all excited components contribute with about 1%. The main contributions come from the projected prolate and oblate states. This situation changes completely for the second  $0^+$ . Here the main contribution comes from the quasiparticle states, where the prolate proton states are dominant.

In the present model it turns out that the deep lying first excited  $0^+$  can only be explained by a coupling of the proton quasiparticle degrees of freedom to the vibrational degrees of freedom. The neutron components are not so important for the lowest energy levels. In comparison with the

experiment one sees that all levels have been calculated in the right order and that there is an overall good agreement.

For  $^{70}\text{Zn}$  and  $^{74}\text{Ge}$  the investigation of the intrinsic binding energies and the pairing energies shows that again the variation after projection and the use of HFB states is indispensable. The method of selection of the generating wave functions and quasiparticles is the same as has been described in the case of  $^{72}\text{Ge}$ . The results obtained for  $^{70}\text{Zn}$  and  $^{74}\text{Ge}$  are given in Fig. 5 and Fig. 6, respectively. In the second columns the projected spectra of a two-quasiparticle excited HFB state (P2qp) are displayed. One recognizes that the spins are not monotonically ordered so that the lowest spins have a very high excitation energy, whereas some higher spins, especially the  $8^+$  for  $^{70}\text{Zn}$  and the  $6^+$  for  $^{74}\text{Ge}$  come rather low. Therefore these projected states will influence essentially the higher spins in a GCM+QP

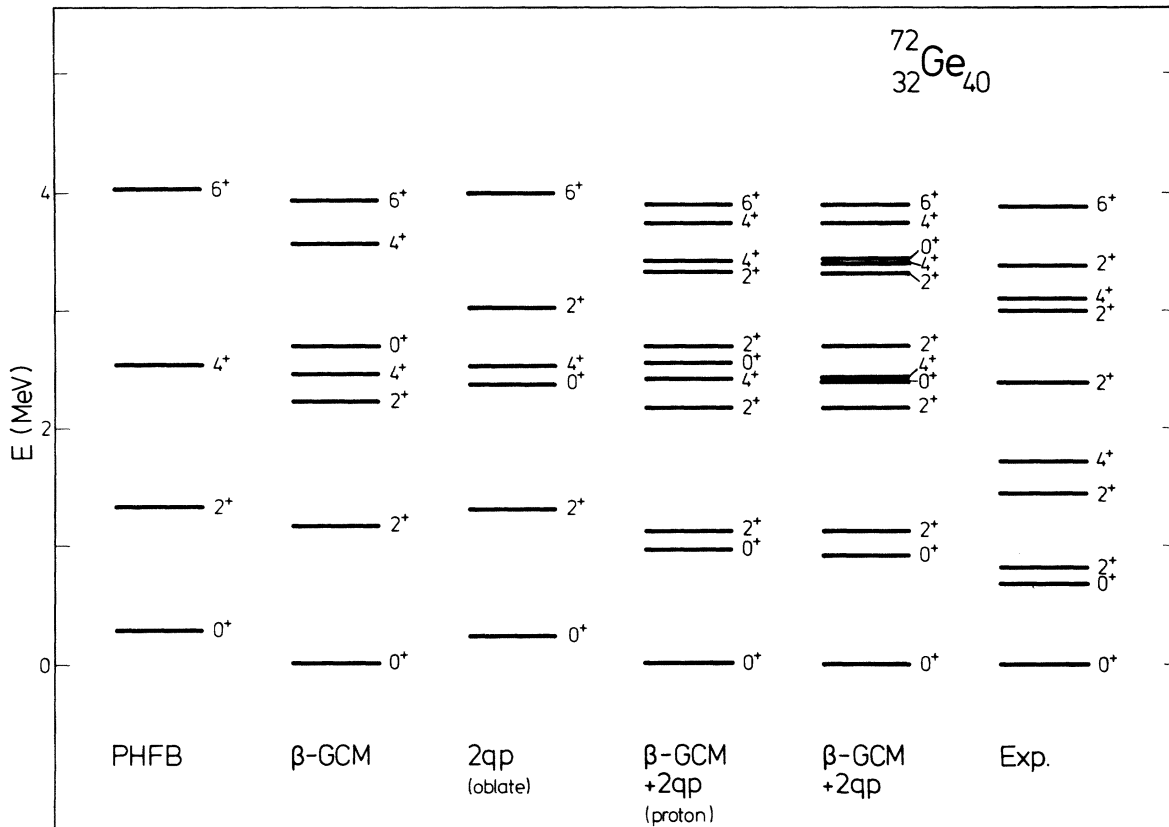


FIG. 3. Comparison of successive GCM+QP calculations for  $^{72}\text{Ge}$  with experiment. PHFB denotes the angular momentum and particle number projected spectrum with a variation of the deformation after projection. The next spectrum ( $\beta$ -GCM) is obtained by a mixing of the two prolate and oblate projected HFB minima. The result of a mixing of all two-quasiparticle excited oblate states with the zero-quasiparticle oblate ground state is given in the third column. The next spectrum [ $\beta$ -GCM+2qp (proton)] results from a mixing of the collective components with all proton two-quasiparticle excited states. ( $\beta$ -GCM+2qp) contains in addition to the previous spectrum one neutron two-quasiparticle excited state (total wave function). The last spectrum (Exp.) shows the experimental data.

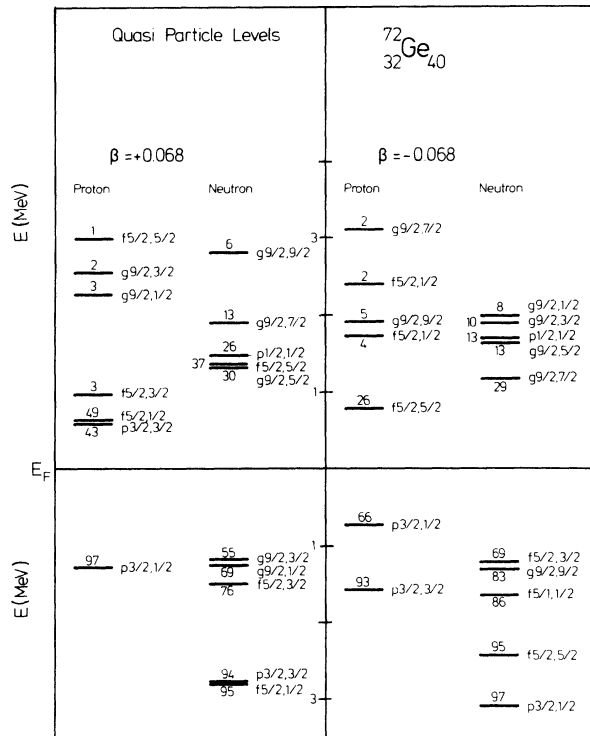


FIG. 4. On the left side one finds the quasiparticle levels of the prolate HFB state at the deformation  $\beta$  where the  $0^+$  binding energy exhibits a minimum. On the right side there are the quasiparticle levels of the corresponding oblate HFB state.  $E_F$  is the Fermi surface.

calculation, as can be seen in the fifth columns. Other projected quasiparticle states show spectra with relatively low lying  $0^+$  states which will contribute to the low lying excitation spectrum.

It is interesting to see that in the case of  $^{70}\text{Zn}$  the relatively low position of the first excited  $0^+$  is mainly caused by the neutron quasiparticle excitations (see column 5, Fig. 5) in contrast to the results in  $^{72}\text{Ge}$ .

A comparison of the final GCM+QP spectra ( $\beta$ -GCM+2qp, Figs. 5 and 6) with the experimental data shows a qualitative agreement for  $^{74}\text{Ge}$  and

$^{70}\text{Zn}$ . In order to get a better quantitative agreement one may multiply the calculated spectra with a scaling factor of 0.8 for  $^{70}\text{Zn}$  and 0.5 for  $^{74}\text{Ge}$ . The reason for the particularly large discrepancy in  $^{74}\text{Ge}$  may be that the effective Hamiltonian fitted for lighter nuclei is not appropriate.

$B(E2)$  values for  $^{72}\text{Ge}$  and  $^{70}\text{Zn}$  are listed in Table II. It was possible to fit simultaneously the  $2_1^+ \rightarrow 0_1^+$ ,  $2_2^+ \rightarrow 2_1^+$ , and  $2_2^+ \rightarrow 0_1^+$  transitions in  $^{72}\text{Ge}$  and the  $2_1^+ \rightarrow 0_1^+$  transition in  $^{70}\text{Zn}$  with only one set of effective charges  $\Delta e_p = 0.8$  and  $\Delta e_n = 0.9$ . Although no unique experimental value could be assigned to the  $2_1^+ \rightarrow 0_2^+$  transition in  $^{72}\text{Ge}$ , it seems to have strong collective components which could not be reproduced in our calculations. A detailed analysis of the different transition matrix elements defined by the components of the total GCM+QP wave function shows that the biggest absolute values for the single transition matrix elements are given by the admixture of the two different deformations of minimal projected energy for the 0 qp states, but they cancel because of different signs. Only the components containing quasiparticle excited wave functions sum up coherently, but their absolute values are by a factor 0.1 to 0.01 smaller than the collective terms. In a stability test one sees that by increasing the space, all transitions, but the  $2_1^+ \rightarrow 0_2^+$ , remain stable within 1% or less. Only the  $2_1^+ \rightarrow 0_2^+$  transition increases by about 300%. This demonstrates the well known fact that stability with respect to the energies does not yet guarantee stable transitions. A common feature for the transitions in both nuclei is that the intraband transitions  $[J_\alpha \rightarrow (J-2)_\alpha]$  are much more collective than the interband transitions  $[J_\alpha \rightarrow (J-2)_{\alpha'}; \alpha \neq \alpha']$ .

#### IV. SUMMARY AND CONCLUSION

In the present investigations, we tried to describe in a fully microscopic way properties of nuclei by coupling quasiparticle degrees of freedom to the collective motion of the nucleons. This aim could be reached by adding  $K=0$  two-quasiparticle excited HFB states to collective states

TABLE I. Analysis of  $0^+$ -wave functions in  $^{72}\text{Ge}$ . The percentage with which the different GCM+QP components contribute to the total GCM+QP wave function is given for  $J=0_1^+$  and  $J=0_2^+$ . P and O designate prolate and oblate states, respectively. p1 is the proton quasiparticle level nearest the Fermi surface  $E_F$ , and so on, n1 is the neutron quasiparticle level nearest the Fermi surface, and so on.

	P	O	P(p1) (p <sub>3/2, 3/2</sub> )	O(o1) (o <sub>3/2, 1/2</sub> )	P(p2) (f <sub>5/2, 1/2</sub> )	O(o2) (f <sub>5/2, 5/2</sub> )	P(n5) (p <sub>1/2, 1/2</sub> )
$0_1^+$ (%)	46.0	52.0	0.01	0.9	0.01	1.2	0.0
$0_2^+$ (%)	2.6	11.5	33.2	7.8	30.3	6.0	8.7

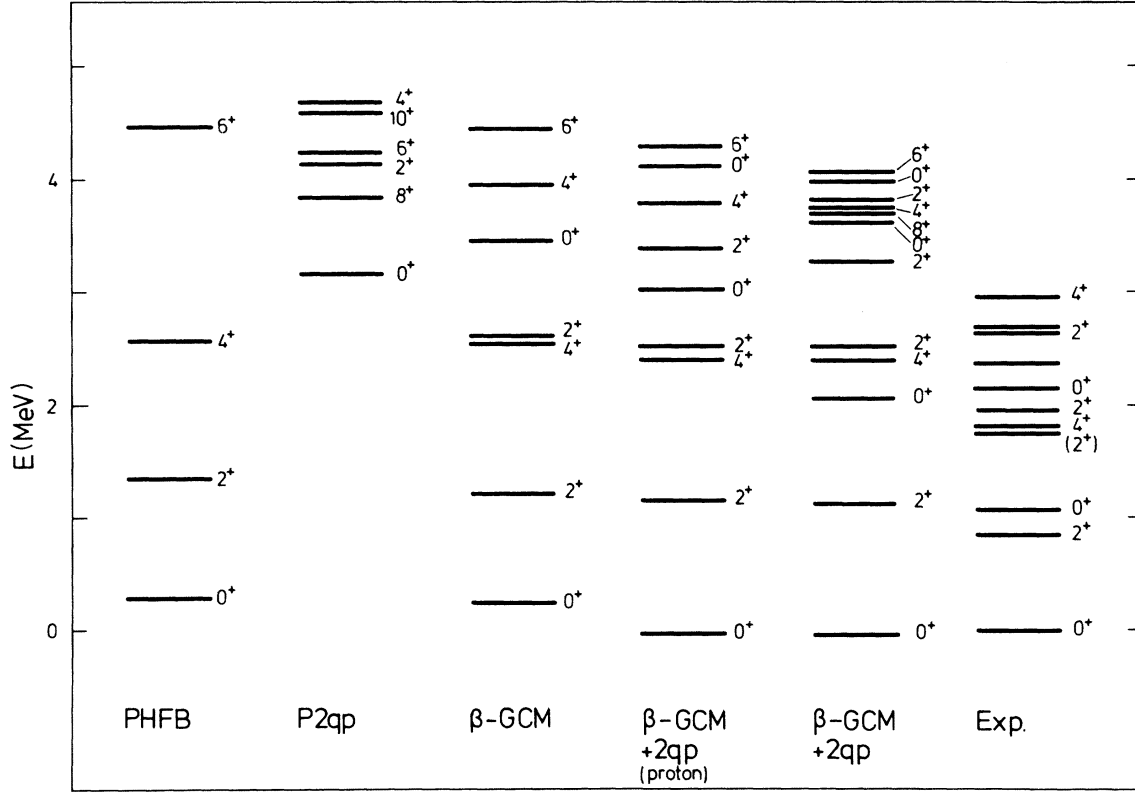


FIG. 5. Comparison of successive GCM+QP calculations for  $^{70}\text{Zn}$  with experiment. PHFB is the minimized angular momentum and particle number projected spectrum. The next spectrum (P2qp) results from a projections of a two-quasiparticle excited HFB state. In the third column ( $\beta$ -GCM) the levels are obtained by a mixing of the two zero-quasiparticle prolate and oblate projected ground states. The following spectrum [ $\beta$ -GCM + 2qp (proton)] includes the two nonexcited prolate and oblate states as well as all proton two-quasiparticle excited states. ( $\beta$ -GCM + 2qp) contains in addition to the previous spectrum some neutron two-quasiparticle excited states (total wave function). The last spectrum (Exp.) shows the experimental data.

TABLE II. Electromagnetic transitions in  $^{72}\text{Ge}$  and  $^{70}\text{Zn}$ .  $BE2$  values for  $^{72}\text{Ge}$  and  $^{70}\text{Zn}$  are given between the initial state  $J_i$  and the final state  $J_f$ , whose energies are denoted by  $E_i$  and  $E_f$ , respectively. Calculated values (GCM+QP) are compared with the experimental ones (Exp.).

$J_i$	$J_f$	$^{72}\text{Ge}$			$^{70}\text{Zn}$		
		$E_i/E_f(\text{GCM+QP})$ (MeV)	$B(E2)(\text{GCM+QP})$ ( $e^2\text{fm}^4$ )	$B(E2)(\text{Exp.})$ ( $e^2\text{fm}^4$ )	$E_i/E_f(\text{GCM+QP})$ (MeV)	$B(E2)(\text{GCM+QP})$ ( $e^2\text{fm}^4$ )	$B(E2)(\text{Exp.})$ ( $e^2\text{fm}^4$ )
$2_1^+$	$0_1^+$	1.13/0.0	482	$440 \pm 50^a$ ; $234^b$	1.15/0.0	333	$320 \pm 28^a$
$4_1^+$	$2_1^+$	2.43/1.13	681		2.43/1.15	390	
$6_1^+$	$4_1^+$	3.90/2.43	740		4.10/2.43	114	
$8_1^+$	$6_1^+$	5.54/3.90	739		3.77/4.10	316	
$10_1^+$	$8_1^+$	7.29/5.54	665		4.57/3.77	433	
$2_1^+$	$0_2^+$	1.13/0.94	9.8	$400 \pm 70^a$ ; $51 \pm 5^c$ $264 \pm 48^d$ ; $370 \pm 48^d$ ;	1.15/2.09	1.4	
$2_2^+$	$0_1^+$	2.18/0.0	18.4	$1.5^b$	2.56/0.0	4.5	
$2_2^+$	$2_1^+$	2.18/1.13	623	$711^b$	2.56/1.15	346	
$4_1^+$	$2_2^+$	2.43/2.18	5		2.43/2.56	70	

<sup>a</sup> See Ref. 13.

<sup>b</sup> See Ref. 14.

<sup>c</sup> See Ref. 15.

<sup>d</sup> See Ref. 16.

described by the generator coordinate method (GCM). The generating wave functions were Hartree-Fock-Bogoliubov states (HFB), constrained to different quadrupole moments. The use of HFB states rather than Hartree-Fock states (HF) was indispensable, because the pairing correlations of the discussed nuclei ( $^{72}\text{Ge}$ ,  $^{70}\text{Zn}$ , and  $^{74}\text{Ge}$ ) could not be neglected. These states have been projected onto angular momentum  $J$  and also on particle number  $N$ . The intrinsic binding energy surfaces are rather shallow for small deformations  $\beta$ . In the procedure of variation after projection, however, two distinct prolate and oblate minima were found for all spins at nearly the same deformation. Projected states with these deformations were used to span the GCM and GCM+QP wave functions. The good agreement of the resulting GCM+QP spectra with experiment demonstrates that the low lying excited levels of the considered nuclei are dominated by the coupling of quasiparticle excitations to shape vibrations. A detailed analysis shows that most of the yrast states are already well described by pure shape vibrations. On the other hand, particularly for the low lying  $0_2^+$  states, which can hardly be

understood in a pure phenomenological model, the mixing between quasiparticle and shape vibrational degrees of freedom turned out to be necessary for a reasonable description. In  $^{72}\text{Ge}$ , for instance, the main contribution (90%) for this state came from the quasiparticle components, among which the proton excitations were the most important ones. In the case of  $^{70}\text{Zn}$ , the greater influence was caused by the neutron excitations.

The spectrum of  $^{74}\text{Ge}$  was in worse agreement with experiment, possibly caused by the effective Hamiltonian which has been fitted to lighter nuclei by Glaudemans and collaborators.

For the  $B(E2)$  values too, we got a rather good agreement with the experimental data, using one common set of small effective charges for all nuclei. For the  $2_1^+ \rightarrow 0_2^+$  transition in  $^{72}\text{Ge}$ , the present description seemed not to contain enough two-quasiparticle components to build up a collective transition.

Another shortcoming of the model presented here is the fact that the  $\gamma$  deformation degree of freedom is not included. The theoretical formulation of the model may be easily generalized to include this degree of freedom. But numerically

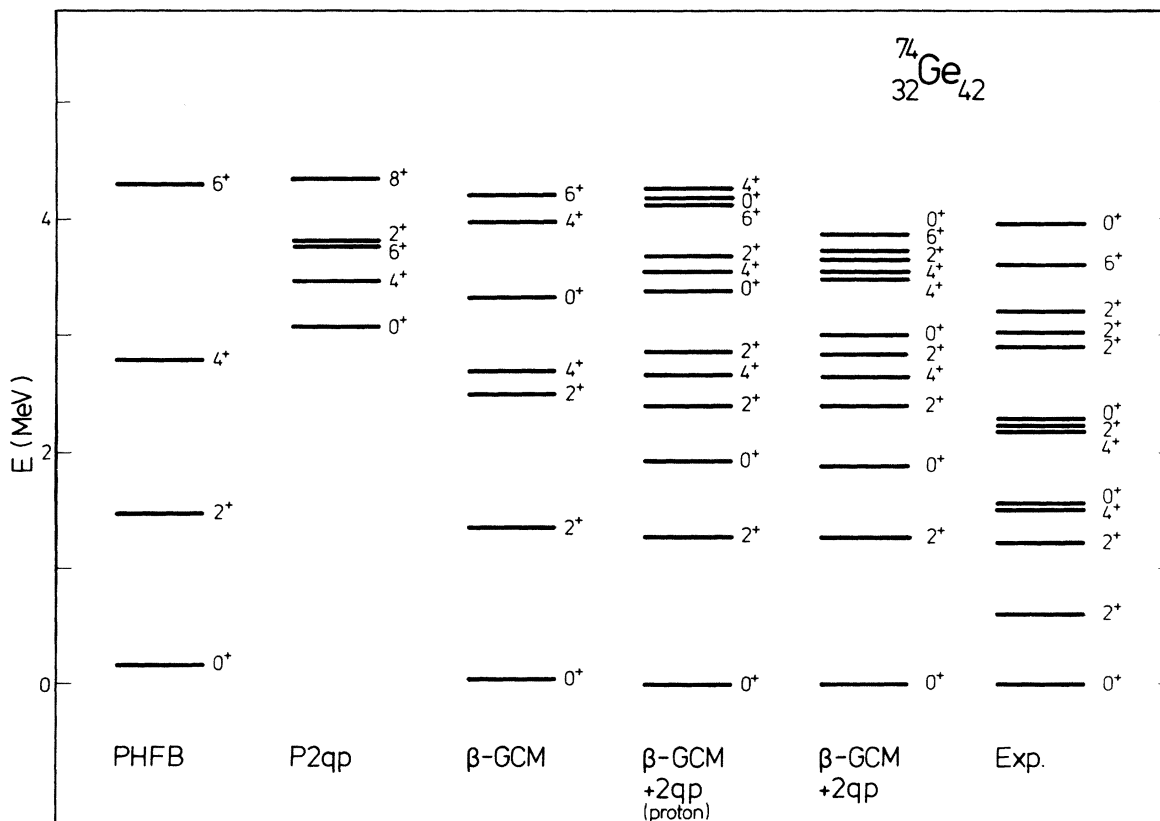


FIG. 6. Comparison of different GCM+QP calculations for  $^{74}\text{Ge}$  with experiment. The details are the same as in Fig. 5.



the calculations are getting too lengthy since the angular momentum projection requires the numerical integrations over all three Euler angles. One expects that this degree of freedom affects the second  $2^+$  states and higher lying levels.

Nevertheless, we can conclude that the GCM+QP method is flexible enough to describe nuclei whose low lying spectra are dominated

simultaneously by a few collective and single particle components. The resulting microscopic nuclear wave function can easily be analyzed to study the influence of the different degrees of freedom on nuclear properties.

One of us (K.G.) thanks B. Castel for fruitful discussions during his stay at Queen's University.

\*University of Bonn, D-5300 Bonn, West Germany.

<sup>1</sup>D. L. Hill, J. A. Wheeler, *Phys. Rev.* **89**, 1102 (1953); J. J. Griffin, J. A. Wheeler, *ibid.* **108**, 312 (1957).

<sup>2</sup>R. E. Peierls and J. Yoccoz, *Proc. Phys. Soc. London* **A70**, 381 (1957); E. Caurier, B. Bourotte-Bilwes, and Y. Agrall, *Phys. Lett.* **44B**, 411 (1973); N. Mankoc-Borstnik, M. V. Mihailovic, and M. Rosina, *Nucl. Phys.* **A239**, 321 (1975); D. Justin, M. V. Mihailovic, and M. Rosina, *ibid.* **A182**, 54 (1972); C. D. Siegal and R. A. Sorensen, *ibid.* **A184**, 81 (1972); K. Goeke, M. V. Mihailovic, K. Allaart, and A. Faessler, *ibid.* **A243**, 440 (1975); K. Allaart, K. Goeke, H. Müther, and A. Faessler, *Phys. Rev. C* **9**, 988 (1974); F. Grümmer, K. W. Schmid, and A. Faessler, *Z. Phys.* **A275**, 391 (1975).

<sup>3</sup>K. Goeke, K. Allaart, H. Müther, and A. Faessler, *Z. Phys.* **271**, 377 (1974).

<sup>4</sup>H. Müther, K. Allaart, K. Goeke, and A. Faessler, *Nucl. Phys.* **A248**, 451 (1975).

<sup>5</sup>H. Müther, K. Goeke, A. Faessler, and K. Allaart, *Phys. Lett.* **60B**, 427 (1976).

<sup>6</sup>M. Kregar and M. V. Mihailovic, *Nucl. Phys.* **A93**, 402 (1967).

<sup>7</sup>B. Castel, M. Micklinghoff, and I. P. Johnstone, *Can.*

*J. Phys.* **51**, 2403 (1973).

<sup>8</sup>B. F. Bayman, A. S. Reiner, and R. K. Sheline, *Phys. Rev.* **115**, 1627 (1959).

<sup>9</sup>K. Goeke, J. Garcia, and A. Faessler, *Phys. Lett.* **41B**, 557 (1972).

<sup>10</sup>K. Allaart, K. Goeke, and A. Faessler, *Z. Phys.* **263**, 407 (1973).

<sup>11</sup>P. W. M. Glaudemans, Fysisch Laboratorium, Rijksuniversiteit Utrecht, private communication.

<sup>12</sup>S. K. Sharma and S. B. Khadkikar, in *Proceedings of the International Conference on Nuclear Physics, Munich, 1973*, edited by J. de Boer and H. J. Mang (North-Holland, Amsterdam/American Elsevier, New York, 1973), Vol. 1; J. K. Parikh, *Phys. Rev. C* **5**, 153 (1972); H. Chandra and M. L. Rustgi, *ibid.* **4**, 874 (1971).

<sup>13</sup>A. C. Rester, J. H. Hamilton, and A. V. Ramayya, *Nucl. Phys.* **A162**, 481 (1971); P. H. Stelson and L. Grodzins, *Nucl. Data* **1A**, 21 (1965).

<sup>14</sup>W. G. Monahan and R. G. Arns, *Phys. Rev.* **184**, 1135 (1969).

<sup>15</sup>M. Kregar and B. Elbek, *Nucl. Phys.* **A93**, 49 (1967).

<sup>16</sup>R. C. Haight, *Phys. Rev. C* **5**, 1984 (1972).